Collision-induced double resonance studies of HN_2^+ and HCN

C. J. Pursell,[a] D. P. Weliky,[b] and T. Oka
Department of Chemistry and Department of Astronomy and Astrophysics, The University of Chicago, Chicago, Illinois 60637

(Received 31 May 1990; accepted 1 August 1990)

We have investigated collision-induced rotational transitions of HN_2^+ and HCN using infrared-microwave four-level double resonance spectroscopy. These two isoelectronic molecules were studied in collisions with He, Ar, and N_2. For all cases studied, we have observed that the collision-induced rotational transitions exhibit collisional "selection rules." The selection rules can be explained using the symmetry properties (i.e., parity) of the dominant terms in the interaction potential. This represents the first observation of selection rules for rotational energy transfer of a molecular ion. This study has allowed us to directly compare the difference between ion–neutral and neutral–neutral collisions which cause rotational transitions. We have experimentally observed that ion–neutral and neutral–neutral collisions differ because of the presence of the Langevin force in the ion–neutral interaction potential, which has two unique effects. The Langevin force produces a charge-induced dipole in the collision partner which is parallel to the ion's electric field. This charge-induced dipole interacts with the electric charge of the molecular ion which creates an attractive force between the ion and neutral. This interaction therefore decreases the ion–neutral distance and produces strong collisions which randomizes the rotational states. The second effect occurs when the molecular ion has a permanent electric moment. The charge-induced dipole in the collision partner will interact with an electric moment of the molecular ion creating a long-range interaction. For HN_2^+, a molecular ion with a permanent dipole moment, this interaction produces "dipole-type" collisional selection rules.

I. INTRODUCTION

Starting with the early work of collisional line broadening in microwave absorption spectroscopy,[1-3] great interest has developed in the study of collision-induced rotational transitions.[4-6] As a result of an inelastic collision, a molecule that is initially in rotational state J_i will be transferred to state J_f. The collisional line broadening (i.e., pressure broadened linewidth) in microwave absorption spectroscopy is related to the total rate at which molecules leave rotational state J_i due to collisions. There are two limiting cases of molecular collisions, strong and weak collisions. In a strong collision the impact is so violent that the final rotational state is independent of the initial state. The final rotational state J_f is selected in accordance with the Boltzmann distribution law. A strong collision may be defined as a collision where the impact parameter (i.e., distance of closest approach) is less than the sum of the van der Waal's radii. However, in a weak collision the initial and final rotational states bear a definite relationship to each other. A weak collision is one in which two molecules pass each other with an impact parameter greater than the sum of the van der Waal's radii. During such a weak collision the change in rotational state is produced by the angular dependent part of the long-range interaction of the electric moments. The relationship between the initial and final rotational state, i.e., the collisional "selection rules," is determined by the symmetry properties of the long-range interaction potential.

In order to study the relationship between J_i and J_f for weak collisions it is necessary to monitor the quantum states i and f independently. This has been done in a variety of ways but microwave–microwave four-level double resonance spectroscopy seems to have been the most productive.[7-9] Four-level double resonance spectroscopy has demonstrated rather clearly that the collision-induced rotational transitions from state J_i to state J_f exhibit selection rules similar to those for radiative transitions. These experimentally observed collisional selection rules contain information about the angular dependent part of the long-range interaction potential that causes the rotational transitions.[8] With the development of infrared lasers, collision-induced rotational transitions have also been studied with infrared-microwave four-level double resonance spectroscopy.[10] In this paper we present our studies of collision-induced rotational transitions using infrared-microwave four-level double resonance spectroscopy. We have previously reported the initial observation of four-level and three-level double resonance spectroscopy of HN_2^+.[11,12] We have investigated the collisions of the isoelectronic species HN_2^+ and HCN with He, Ar, and N_2. In all cases studied, we have observed collisional selection rules. These experimentally observed collisional selection rules have yielded information concerning the angular dependent part of the interaction potential. The results for collisions of HN_2^+ and HCN with He have been compared with the theoretical studies of collision-induced rotational transitions of molecular ions by Green.[13,14] Apart from Katayama's work on collisions of N_2^+ with He in which he observed J specificity in rovibronic energy transfer,[15] this

[a] Present address: Department of Chemistry, Indiana University, Bloomington, IN 47405.
[b] NSF Predoctoral Fellow.

 0021-9606/90/227041-08$03.00

represents the first observation of selection rules for rotational energy transfer of a molecular ion.

This study has allowed us to directly compare the difference between ion–neutral and neutral–neutral collisions which cause rotational transitions. The ion–neutral collision is qualitatively different from the neutral–neutral collision because of the presence of the long-range Langevin force in the interaction potential.[16,17] Because of the Langevin force, it was initially believed that the rate of rotational transitions in ion–neutral collisions would be 20 to 30 times faster than in neutral–neutral collisions.[18,19] This implied that the pressure broadened linewidths of molecular ions would be so large as to make observation of the ion's microwave spectra impossible. However, the successful laboratory observation of the microwave spectra of CO^+, HCO^+, and HN_2^+ by Woods and his co-workers discredited such fast collision-induced rotational transition rates.[20] These studies[20] along with measurements of the pressure broadening of HCO^+ by H_2 (Refs. 21,22) indicate that the rate of rotational transitions in molecular ion–neutral collisions are only a few times (cf. 3–4) larger than those in neutrals.

Our studies presented in this paper demonstrate that ion–neutral and neutral–neutral collisions differ because of the presence of the Langevin force in the ion–neutral interaction potential, which has two unique effects. The Langevin force produces a charge induced dipole in the collision partner which is parallel to the ion's electric field. This charge-induced dipole interacts with the electric charge of the molecular ion which creates an attractive force between the ion and neutral. This interaction therefore decreases the ion–neutral distance and produces strong collisions which randomizes the rotational states. The second effect occurs when the molecular ion has a permanent electric moment. The charge induced dipole in the collision partner interacts with an electric moment of the molecular ion creating a long-range interaction. For HN_2^+, a molecular ion with a permanent dipole moment, this interaction produces "dipole-type" collisional selection rules.

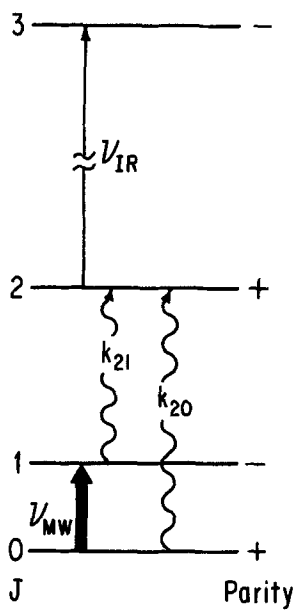

FIG. 1. The four-level system for infrared-microwave double resonance spectroscopy. The gas sample is simultaneously irradiated with low power infrared radiation (probe) and high power microwave radiation (pump). When the microwave frequency is resonant with the molecular transition $J = 1 \leftarrow 0$, the microwave radiation saturates the molecular transition. This perturbation of the populations from equilibrium will be transferred to other rotational levels by rotationally inelastic collisions. The infrared radiation is then used to probe the molecular population to the rotational levels, $J = 2,3,4...$. The four-level double resonance signal is observed when the molecular population transfer *obeys* selection rules. In other words, a collision-induced double resonance signal is observed when one collisional path is preferred over another. For example the transfer of molecules to $J = 2$ will be observed when either k_{21}, the rate constant for dipole-type transitions, or k_{20}, the rate constant for quadrupole-type transitions, is greater than the other, where k_{fi} is the collisional rate constant.

II. THEORY

We have used infrared-microwave four-level double resonance spectroscopy to study collision-induced transitions between rotational levels[8] in the ground vibrational state of HN_2^+ and HCN. The four-level double resonance system is shown in Fig. 1. The gas sample is simultaneously irradiated with low power infrared radiation (probe) and high power microwave radiation (pump). When the microwave frequency is resonant with the rotational transition $J = 1 \leftarrow 0$, the microwave radiation saturates the molecular transition (i.e., the radiation is of sufficient intensity to cause molecules to be transferred from $J = 0$ to $J = 1$). This perturbation of the populations from equilibrium will be transferred to other rotational levels by rotationally inelastic collisions. The infrared radiation is then used to probe the population transfer to the rotational levels, $J = 2,3,4...$. The four-level double resonance signal is observed when the molecular population transfer *obeys* selection rules. In other words, a collision-induced double resonance signal is observed when one collisional path is preferred over another. For example the transfer of molecules to $J = 2$ in Fig. 1 will be observed when either k_{21}, the rate constant for "dipole-type" transitions, or k_{20}, the rate constant for "quadrupole-type" transitions, is greater than the other, where k_{fi} is the collisional rate constant.

With full microwave saturation the variation of the population in the pumped rotational levels is

$$\delta n_1 = -\delta n_0 = (n_0^0 - n_1^0/3)/2 \approx n_0^0 (h\nu_{10}/2kT), \qquad (1)$$

where δn_i is the population variation in the rotational level $i = J$, and n_i^0 is the equilibrium value. The factor of 3 comes from the degeneracy of the $J = 1$ state. Because δn_i is small (cf. $\delta n_i/n_i^0 \sim 1\%$), we can use linear rate equations.[8] Without the microwave pump radiation we have

$$\sum_i (k_{fi} n_i^0 - k_{if} n_f^0) = \dot{n}_f \equiv 0, \qquad (2)$$

where k_{fi} is the rate constant for population transfer from i to f. Because of the principle of detailed balancing,

$$k_{fi}/k_{if} = n_f^0/n_i^0 \qquad (3)$$

and the individual expressions in the brackets in Eq. (2) are zero. Under the continuous application of the microwave pump radiation, we have

$$\sum_i (k_{fi}n_i - k_{if}n_f) + R(\delta_{f1} - \delta_{f0})(n_0 - n_1/3) = \dot{n}_f \equiv 0, \tag{4}$$

where δ_{f1} and δ_{f0} are Kronecker's delta and R is the rate constant of radiative transitions with strong microwave radiation. However, because we assume full microwave saturation with $\delta n_1 = -\delta n_0, n_0 - n_1/3 = 0$ in Eq. (4). Therefore for values of f, other than $f = 0$ and 1, we obtain by subtracting Eq. (2) from Eq. (4),

$$\sum_i (k_{fi}\delta n_i - k_{if}\delta n_f) = \delta\dot{n}_f = 0 \quad (f \neq 0,1). \tag{5}$$

Equation (5) has an infinite number of k_{fi}'s and is not applicable to practical problems. We therefore make the approximation to retain only δn_i terms in Eq. (5) with $i < f$. This approximation is based on the idea that we directly perturb the population of levels $J = 0$ and 1 and successively consider the population changes in levels $J = 2,3,4...$ assuming all other levels work as a thermal bath. This is reasonable because δn_0 and δn_1 are much larger in magnitude than δn_i ($i \neq 0,1$). Therefore for $f = 2$ (rotational state $J = 2$) Eq. (5) is

$$k_{20}\delta n_0 + k_{21}\delta n_1 - \sum_i k_{i2}\delta n_2 = 0. \tag{6}$$

With $\delta n_1 = -\delta n_0$ from Eq. (1), Eq. (6) can be written as

$$\delta n_2/\delta n_1 = \frac{(k_{21} - k_{20})}{k_T}, \tag{7}$$

where $k_T = \sum_i k_{i2}$ is the rate constant which corresponds to the total rate at which molecules are removed from a rotational level to all other possible levels (cf. the pressure broadened linewidth, $\Delta\nu = k_T/2\pi$). Similarly, the population changes in levels $J = 3$ and 4 created by collision can be derived and are

$$\delta n_3/\delta n_1 = \frac{(k_{31} - k_{30})}{k_T} + \frac{(k_{21} - k_{20})}{k_T}\frac{k_{32}}{k_T} \tag{8}$$

and

$$\delta n_4/\delta n_1 = \frac{(k_{41} - k_{40})}{k_T} + \frac{(k_{21} - k_{20})}{k_T}\frac{k_{42}}{k_T} + \frac{(k_{31} - k_{30})}{k_T}\frac{k_{43}}{k_T} + \frac{(k_{21} - k_{20})}{k_T}\frac{k_{32}}{k_T}\frac{k_{43}}{k_T}. \tag{9}$$

In Eqs. (7)–(9) and for $\Delta\nu = k_T/2\pi$, k_T is assumed to be the same for all J. Equation (7) gives the efficiency for transferring molecules to level $J = 2$ from pumping $J = 1 \leftarrow 0$ by the two competing collisional paths, $J = 2 \leftarrow 1$ (k_{21}) and $J = 2 \leftarrow 0$ (k_{20}) (see Fig. 1). If these two paths have comparable rates, $k_{21} \approx k_{20}$, then $\delta n_2 = 0$. However, if one path occurs with a faster rate, then $\delta n_2 \neq 0$ and we observe collision-induced double resonance signals. The sign of $\delta n_2/\delta n_1$ directly gives information about whether $k_{21} > k_{20}$ or whether $k_{20} > k_{21}$. For example, if $\delta n_2/\delta n_1$ is positive then $k_{21} > k_{20}$ and we say that the collision-induced rotational transitions prefer dipole-type transitions, i.e., dipole-type selection rules, $\Delta J = \pm 1$. If $\delta n_2/\delta n_1$ is negative then $k_{20} > k_{21}$ and the collision-induced rotational transitions prefer quadrupole-type transitions, i.e., quadrupole-type selection rules, $\Delta J = \pm 2$. The larger the value of $\delta n_2/\delta n_1$, the more *rigorous* the selection rule. Equations (8) and (9) are more complicated than Eq. (7) because of the greater number of collisional paths (see Fig. 2). For example, from Eq. (8) besides the direct transfer to level $J = 3$ from $J = 1$ (k_{31}, quadrupole-type transitions) and $J = 0$ (k_{30}, "octopole-type" transitions) there is also a contribution from $J = 2$ (k_{32}, dipole-type cascading).

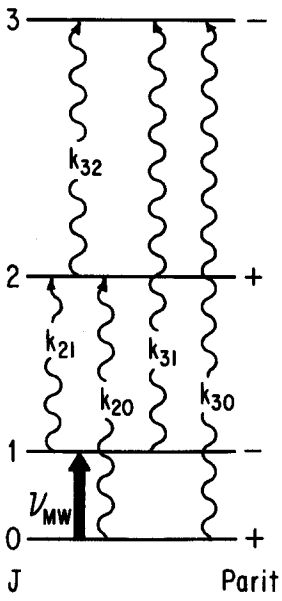

FIG. 2. The energy level system showing all the collisional paths to the $J = 3$ rotational level. This figure shows the collisional paths to the $J = 3$ level by direct transfer of population from $J = 0$ and 1, and by cascading from the $J = 2$ level.

III. EXPERIMENTAL

A detailed description of the infrared-microwave double resonance spectrometer has been given previously.[12] A brief description along with the experimental procedure will be given here. A millimeter wave klystron ($\nu = 87.1$–93.3 GHz, 200–450 mW) is used to pump the $J = 1 \leftarrow 0$ pure rotational transition in the ground vibrational state of HN_2^+ and HCN [cf. $\nu(J = 1 \leftarrow 0) = 93\,173.4$ MHz and 88 631.6 MHz for HN_2^+ and HCN, respectively]. In all cases studied the pressure and modulation are kept large enough to prevent resolving the hyperfine structure in HN_2^+ and HCN. The tunable infrared radiation from a color center laser ($\nu = 3000$–$3600\ cm^{-1}$, 1–25 mW) is used to probe the population changes in the rotational states $J = 1,2,3....$ The double resonance cell is a hollow cathode discharge cell,[12] which services two purposes. First, the hollow cathode discharge is capable of producing relatively large concentrations of ions (cf. 10^{10}–$10^{11} cm^{-3}$) at the low pressures needed for saturation. This point is of course only important for the HN_2^+ case. Second, the circular cathode serves as a waveguide for the propagation of the microwave radiation.

The experiments are performed as follows. The infrared frequency is adjusted to the peak of the Doppler-broadened infrared transition $\nu_1 R(J)$, with $J = 1,2,3...$. The infrared power is kept low to prevent it from saturating the molecular transition. Throughout the experiments the infrared and mi-

crowave power are kept constant. The frequency of the microwave radiation, which is frequency modulated at 100 kHz, is then swept. The infrared power is monitored at the modulation frequency of the microwave radiation using phase sensitive detection. The double resonance signal is observed as a change in the infrared absorption δI_J when the microwave radiation is resonant with the rotational transition $J = 1 \leftarrow 0$. The infrared radiation is therefore a probe of the population transfer. However, because the intensity of $\nu_1 R(J)$ changes with J, the probe of the population transfer also changes. We therefore "normalize" all δI_J by dividing by the intensity of $\nu_1 R(J)$, i.e., $\delta I_J / I_J^0 \equiv \delta n_J / n_J^0$ where I_J^0 is the infrared intensity of $\nu_1 R(J)$ without microwave pumping. Also, with Eqs. (7)–(9) in mind, we divide all $\delta n_J / n_J^0$ by $\delta n_1 / n_1^0$, i.e., we divide the intensity of the collision-induced four-level double resonance signals by the intensity of the direct three-level double resonance signal. We therefore assume that the three-level and four-level double resonance signals depend on the population in the same way. We report the collision-induced signals as $(\delta n_J / \delta n_1) \times 100\%$, where it is understood that δn_J has been normalized by n_J^0. Each signal is measured at least three times, and the error is estimated to be $\pm$ 10% of $[(\delta n_J / \delta n_1) \times 100\%]$.

For collisions of HN_2^+ the discharge conditions are as follows. With liquid-N_2-cooling of the cathode, we add 15–20 mTorr of H_2 and then enough N_2 to start the discharge. The $H_2 + N_2$ total pressure is reduced to 20 mTorr. The collision partner is then added to make the final pressure 220–240 mTorr. Increasing the pressure to 300 mTorr does not affect the relative signal intensities. We therefore believe that the collisions of HN_2^+ are predominately with the collision partner and not excess H_2 and N_2. The rotational temperature is observed to be $\sim$200 K, and the translational temperature is estimated to be $\sim$100–200 K. For more details of the hollow cathode discharge see Ref. 12.

For collisions of HCN no discharge is used but the hollow cathode is still used as the gas cell. With no cooling, approximately 2 mTorr of HCN are added. The collision partner is then added to make the final pressure 200 mTorr. The collisions of HCN are therefore predominately with the collision partner. The rotational and translational temperatures are assumed to be 300 K.

IV. RESULTS AND ANALYSIS

The results for the collision-induced double resonance of HN_2^+ with He, Ar, and N_2 are listed in Table I. The results for collisions of HCN with He, Ar, and N_2 are listed in Table II. The clearest demonstration of the difference between ion–neutral and neutral–neutral collisions that we have observed are plotted in Figs. 3 and 4. The results for HN_2^+ and HCN with He in Fig. 3 show the remarkable difference between the preferred dipole-type rotational transitions of the ion and the preferred quadrupole-type rotational transitions of the isoelectronic neutral. The results for HN_2^+ and HCN with N_2 in Fig. 4 show a qualitatively similar preference for dipole-type rotational transitions of the ion and neutral. These results will be discussed further below. The following discussion and analysis are based on the linear rate equations, Eqs. (7)–(9).

We shall discuss the results for HN_2^+ collisions with He, Ar, and N_2 first. From Table I we see that all of the collision-

TABLE I. Collision-induced double resonance signals of HN_2^+ $(\delta n_J / \delta n_1 \times 100\%)$.[a]

J	He	Ar	N_2
2	6.5	3.2	5.3
3	1.9	0.9	1.2
4	1.2	0.6	0.4

[a] Relative intensities of at least three measurements with an uncertainty of $\pm$ 10% (i.e., the signal for He $J = 2$ is $6.5 \pm 0.6\%$).

TABLE II. Collision-induced double resonance signals of HCN $(\delta n_J / \delta n_1 \times 100\%)$.[a]

J	He	Ar	N_2
2	− 16.4	− 2.5	10.0
3	14.0	2.0	2.7
4	− 12.0	− 1.7	0.9
5	10.0	1.5	
6	− 5.1	− 0.8	
7	3.9	0.4	
8	− 2.8	− 0.2	
9	2.2		
10	− 3.0		
11	1.2		
12	− 0.8		
13	0.6		

[a] Relative intensities of at least three measurements with an uncertainty of $\pm$ 10% (i.e., the signal for He $J = 2$ is $-16.4 \pm 1.6\%$).

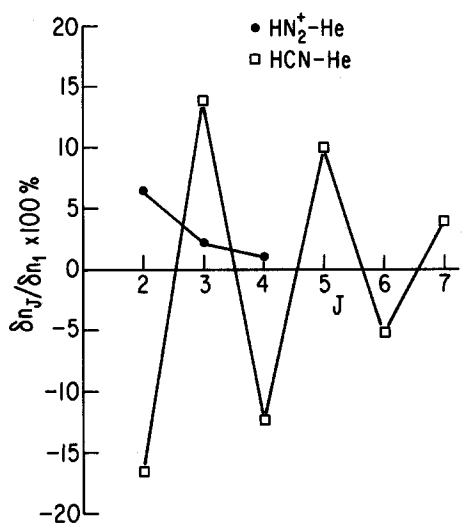

FIG. 3. A plot of the collision-induced double resonance signals for the collisions of HN_2^+ and HCN with He. The results show a dramatic difference between ion–neutral and neutral–neutral collisions. The zig-zag nature of the HCN–He collisional results demonstrate a strong preference for quadrupole-type rotational transitions, while the monotonically decreasing nature of the HN_2^+–He collisional results show a weaker preference for dipole-type rotational transitions.

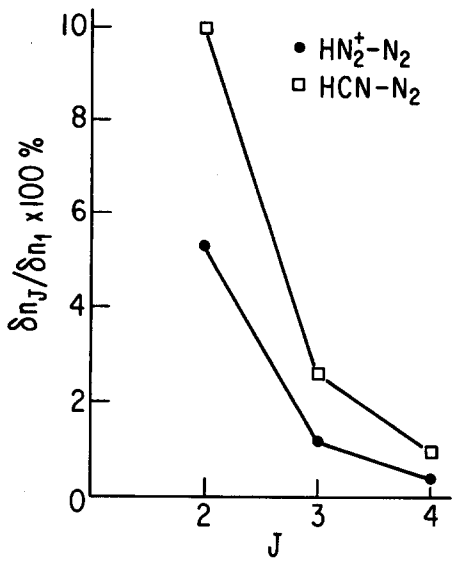

FIG. 4. A plot of the collision-induced double resonance signals for the collisions of HN_2^+ and HCN with N_2. Unlike the dramatic difference in the results shown in Fig. 3, the results are qualitatively very similar. Both HN_2^+ and HCN collisions with N_2 show a similar preference for dipole-type rotational transitions.

induced double resonance signals, $\delta n_J/\delta n_1$, are positive. Using Eq. (7) with $\delta n_2/\delta n_1 > 0$, the results indicate that $k_{21} > k_{20}$. This means that the rotational transitions of HN_2^+ produced by collisions with He, Ar, and N_2 prefer dipole-type transitions. In other words, all of the ion–neutral collisions that we observed exhibit a preference for dipole-type rotational transitions. Using Eq. (7) for $\delta n_2/\delta n_1$ clearly illustrates whether dipole-type or quadrupole-type rotational transitions are preferred. From Table I we also see that the magnitudes of the collision-induced double resonance signals of HN_2^+ with He, Ar, and N_2 are very similar, which suggests that the collisions have a similar preference for dipole-type transitions. From Eq. (7) we note that $\delta n_2/\delta n_1$ is inversely proportional to k_T. It has been experimentally observed that for molecular ions k_T can be equated to the Langevin rate constant, $k_L \propto (\alpha/\mu)^{1/2}$, where α is the polarizability of the collision partner and μ is the collisional reduced mass.[22] The values of k_L for HN_2^+ with He, Ar, and N_2 are very similar (cf. the ratio of k_L for HN_2^+ with He, Ar, and N_2 is 0.68/0.88/1). Our results then indicate that $(k_{21} - k_{20})$ in Eq. (7) is also very similar for collisions of HN_2^+ with He, Ar, and N_2.

The collision-induced double resonance signals of HCN with He, Ar, and N_2 are listed in Table II. The collisions of HCN with N_2 give $\delta n_2/\delta n_1 > 0$ and from Eq. (7) we again see that $k_{21} > k_{20}$. Therefore the collisions of HCN with N_2 prefer dipole-type rotational transitions, and are qualitatively similar to the collisions of HN_2^+ with He, Ar, and N_2. The results for collisions of HCN with He and Ar are qualitatively similar and very different from all the other collisional cases. Since $\delta n_2/\delta n_1$ is negative, we would conclude that $k_{20} > k_{21}$ in Eq. (7). Therefore the collisions of HCN with He and Ar show a preference for quadrupole-type rotational transitions. Contrary to the previous four-level double resonance studies,[8] this is the first time that He and Ar show such similar collisional selection rules. To the best of our knowledge, the zig-zag nature of the results for collisions of HCN with He in Fig. 3 is the clearest demonstration of quadrupole-type collisional selection rules.

We will now discuss the differences between ion–neutral and neutral–neutral collisions which cause rotational transitions. First, we compare the collision-induced double resonance signals of HN_2^+ and HCN with He, as shown in Fig. 3. The difference between ion–neutral and neutral–neutral collisions for this case are dramatic. The zig-zag nature of the HCN–He collisional results demonstrate a strong preference for quadrupole-type rotational transitions, while the monotonically decreasing nature of the HN_2^+–He collisional results show a weaker preference for dipole-type rotational transitions. We can compare these results with those from a fully quantum mechanical calculation of the individual collisional rate constants by Green.[23] The rate constants for collision-induced transitions between discrete J rotational states have been computed at low temperatures, $T \leqslant 40$ K for HN_2^+ collisions with He and $T \leqslant 100$ K for HCN collisions with He.[13,14] These rate constants demonstrate an Arrhenius-type behavior. Therefore using Arrhenius-type plots, we have calculated the individual rate constants at $T = 100$ K for HN_2^+ collisions with He and at $T = 300$ K for HCN collisions with He. These temperature represent our estimated experimental translational temperatures. For example, from Ref. 13 we have plotted $\ln(k_{21})$ vs $1/T$ for $T = 5$, 10, 20, 30, and 40 K for collisions of HN_2^+ with He and then extrapolated in order to determine k_{21} at 100 K. Using Eqs. (7)–(9) and the extrapolated rate constants from the Arrhenius-type plots, we have therefore calculated $\delta n_J/\delta n_1$ for J up to 4, as shown in Table III. In these calculations we have used $k_T = \Sigma_i k_{i0}$ with $i = 1$–6. For HN_2^+ collisions with He at $T = 100$ K $k_T = 8.5 \times 10^{-10}$ cm^3 s^{-1}, and for HCN collisions with He at $T = 300$ K $k_T = 2.6 \times 10^{-10}$ cm^3 s^{-1}. From Table III, the results from an extrapolation of the theoretical rate constants are therefore in good qualitative agreement with our experimental results. For HCN with He, the calculated results suggest a larger preference for quadrupole-type rotational transitions than we observed. However, the overall agreement is very satisfying.

The final comparison we would like to make is for the collisions of HN_2^+ and HCN with N_2 as shown in Fig. 4.

TABLE III. Comparison of experimental and theoretical collision-induced double resonance signals of HCN and HN_2^+ with He ($\delta n_J/\delta n_1 \times 100\%$).

J	HCN–He		HN_2^+–He	
	This work	Calculated[a]	This work	Calculated[a]
2	−16.4	−47.6	6.5	5.7
3	14.0	35.2	1.9	0.6
4	−12.0	−31.1	1.2	0.9

[a] Calculated with Eqs. (7)–(9) using the rate constants from Arrhenius-type plots of the theoretical rate constants from Refs. 13 and 14 for HCN at 300 K and for HN_2^+ at 100 K.

Unlike the dramatic difference in the results shown in Fig. 3, the results shown in Fig. 4 are qualitatively very similar. Quantitatively, from Tables I and II, we see that $\delta n_2/\delta n_1$ (HCN–N_2) $\approx 2\ \delta n_2/\delta n_1$ (HN_2^+–N_2). From Eq. (7), we note that $\delta n_2/\delta n_1$ is proportional to $1/k_T$, which can be estimated from pressure broadened linewidth studies since $\Delta\nu = k_T/2\pi$. This will then allow us to compare $(k_{21} - k_{20})$ from Eq. (7) for ion–neutral and neutral–neutral collisions. There are no reports of linewidths studies of HN_2^+ with N_2, but linewidths studies of HCO^+ with CO have been carried out.[22] Since HCO^+ and HN_2^+ are isoelectronic and have similar dipole moments, and CO and N_2 are isoelectronic, we equate their pressure broadened linewidths (i.e., their pressure broadening parameters, $\Delta\nu_p$, where $\Delta\nu = \Delta\nu_p p$ and p is the pressure). Thus, the pressure broadening parameter of HN_2^+ broadened by N_2 in a liquid-N_2 discharge is $\Delta\nu_p(HN_2^+\text{–}N_2) \approx 16.8$ MHz/Torr.[22] There are no reports of linewidth studies of HCN with N_2, but studies with H_2 have been carried out.[24] At 300 K the pressure broadening parameter for HCN broadened by H_2 is $\Delta\nu_p$ (HCN–H_2) $= 5.0 \pm 0.5$ MHz/Torr.[24] We can scale this to HCN collisions with N_2 by comparing the difference in the pressure broadening of NH_3 with N_2 and H_2 [cf. $\Delta\nu_p(NH_3\text{–}N_2)/\Delta\nu_p(NH_3\text{–}H_2) = 3.8/3.0$].[25] This is reasonable since HCN and NH_3 have relatively similar dipole moments and should exhibit similar pressure broadening behavior. We therefore estimate the pressure broadening parameter of HCN broadened by N_2 to be $\Delta\nu_p$ (HCN–$N_2 \approx 6$ MHz/Torr). We would therefore estimate that

$$\frac{\Delta\nu_p(HN_2^+\text{–}N_2)}{\Delta\nu_p(HCN\text{–}N_2)} \approx 2.8$$

or $k_T(HN_2^+\text{–}N_2) \approx 2.8 k_T(HCN\text{–}N_2)$. This agrees with earlier studies of pressure broadened linewidths of molecular ions,[21,22] in which it was found that the rates of rotational transitions in molecular ion–neutral collisions are only a few times (cf. 3–4) larger than those in neutral–neutral collisions. Using Eq. (7) again and $\delta n_2/\delta n_1$ (HCN–N_2) $\approx 2\delta n_2/\delta n_1$ (HN_2^+–N_2), the above result suggests that the factor of 2 is mostly due to the denominator in Eq. (7). This implies that $(k_{21} - k_{20})$ is comparable for HN_2^+ and HCN collisions with N_2.

V. DISCUSSION

As mentioned in the Introduction, the directly observed selection rules of the collision-induced double resonance signals contain information about the angular dependent part of the long-range interaction potential that causes rotational transitions. The first-order approximation of the transition probability for a collision-induced rotational transition is[8]

$$P(f_1 f_2 \leftarrow i_1 i_2) = \left| 1/\hbar \int_{-\infty}^{+\infty} \langle f_1 f_2 | V(\mathbf{r},\boldsymbol{\Omega}_1,\boldsymbol{\Omega}_2) | i_1 i_2 \rangle \times \exp(i\Delta E t/\hbar) dt \right|^2 \quad (10)$$

where i_1 and i_2 are the initial states and f_1 and f_2 are the final states of molecule one and two, respectively, $V(\mathbf{r},\boldsymbol{\Omega}_1,\boldsymbol{\Omega}_2)$ is the interaction potential, $\mathbf{r}$ is the intermolecular distance, $\boldsymbol{\Omega}_1$ and $\boldsymbol{\Omega}_2$ are the angular coordinates of molecules one and two, respectively, and $\Delta E = \Delta E_1 + \Delta E_2$. Since we are only concerned about the change in the rotational state of molecule one, we only need to consider the symmetry properties of the transition probability with respect to molecule one. Therefore, the matrix elements in Eq. (10) under coordinate inversion (i.e., $-\boldsymbol{\Omega}_1 \leftarrow \boldsymbol{\Omega}_1$, parity of molecule one) must be invariant in order to give a nonzero probability. Thus, if the parity of $V(\mathbf{r},\boldsymbol{\Omega}_1,\boldsymbol{\Omega}_2)$ is (+) then states i_1 and f_1 must have the same parity, i.e., the parity selection rule for the transition is $\pm \leftrightarrow \pm$. If the parity of $V(\mathbf{r},\boldsymbol{\Omega}_1,\boldsymbol{\Omega}_2)$ is (−) then states i_1 and f_1 must have opposite parity, i.e., the parity selection rule is $+ \leftrightarrow -$. Therefore, by observing the collisional selection rules we can determine the dominant terms in the multipole expansion of the potential. We present the dominant terms below, followed by a discussion of the collision-induced double resonance signals and the observed selection rules in light of these interaction terms.

For collisions of the molecular ion HN_2^+ with He, Ar, and N_2 the *Langevin* term (monopole–charge induced dipole) in the potential is

$$V(r)_L = -\frac{\alpha e^2}{r^4}, \quad (11)$$

where α is the polarizability of the collision partner (i.e., He, Ar, or N_2) and e is the electric charge. However, this term has no angular dependence to cause a rotational transition because the induced dipole is parallel to the ion's electric field. The Langevin force also creates a *dipole–charge induced dipole* term $(\mu - \mu_c')$ which is

$$V(\mathbf{r},\boldsymbol{\Omega}_1,\boldsymbol{\Omega}_2)_{\mu-\mu_c'} = -\frac{2e\alpha(\boldsymbol{\mu}\mathbf{r})}{r^6}, \quad (12)$$

where $\boldsymbol{\mu}$ is the dipole moment operator of HN_2^+. The parity of this potential term in Eq. (12) is (−). This term then gives $+ \leftrightarrow -$ parity selection rules. For collisions of HN_2^+ and HCN with He, Ar, and N_2 there is a *dipole–dipole induced dipole* term $(\mu - \mu_d')$ which is

$$V(\mathbf{r},\boldsymbol{\Omega}_1,\boldsymbol{\Omega}_2)_{\mu-\mu_d'} = -\frac{\alpha}{r^6}\left\{\mu^2 + \frac{3}{r^2}(\boldsymbol{\mu}\mathbf{r})^2\right\}, \quad (13)$$

where α is the polarizability of the collision partner and $\boldsymbol{\mu}$ is the dipole moment operator of HN_2^+ (or HCN). The parity of this potential term is (+). This term, Eq. (13), gives $\pm \leftrightarrow \pm$ parity selection rules. For HN_2^+ and HCN collisions with N_2 there is also a *dipole–quadrupole* term $(\mu - Q)$,

$$V(\mathbf{r},\boldsymbol{\Omega}_1,\boldsymbol{\Omega}_2)_{\mu-Q} = \frac{1}{r^5}\left\{\mathbf{r}\mathbf{Q}\boldsymbol{\mu} - \frac{5}{2r^2}(\mathbf{r}\mathbf{Q}\mathbf{r})\mathbf{r}\boldsymbol{\mu}\right\}, \quad (14)$$

where Q is the quadrupole moment tensor of N_2. This term gives $+ \leftrightarrow -$ parity selection rules. The above potential terms and parity selection rules are summarized in Table IV for all the collisional cases.

We shall discuss the results for HN_2^+ collisions with He, Ar, and N_2 first. Again from Table I we see that all of the collision-induced double resonance signals, $\delta n_J/\delta n_1$, are positive, indicating that the collisions of HN_2^+ with He, Ar, and N_2 prefer dipole-type rotational transitions, i.e., dipole-type selection rules, $\Delta J = \pm 1$, or $+ \leftrightarrow -$ parity selection rules. Considering the above interaction potential terms (see

Table IV), we see that the *dipole–charge induced dipole* term, Eq. (12), with $+ \leftrightarrow -$ parity selection rules would account for the observed collisional selection rules for collisions of HN_2^+ with He, Ar, and N_2. The *dipole–quadrupole* term, Eq. (14) with $+ \leftrightarrow -$ parity selection rules would also account for the observed collisional selection rules for collisions of HN_2^+ with N_2. Therefore we conclude that for collisions of HN_2^+ with He and Ar the observed collisional selection rules for rotational transitions are predominantly produced by *dipole–charge induced dipole* interactions. For collisions of HN_2^+ with N_2 the observed selection rules are produced by *dipole–charge induced dipole* interactions and *dipole–quadrupole* interactions, with the actual contribution from each interaction being indeterminable from our experiments.

The collision-induced double resonance signals of HCN with He, Ar, and N_2 are listed in Table II. The collisions of HCN with N_2 give $\delta n_2/\delta n_1 > 0$ and from Eq. (7) we again see that $k_{21} > k_{20}$, indicating a preference for dipole-type rotational transitions. For collisions of HCN with N_2 only the last two interaction terms apply, Eqs. (13) and (14). We see that the *dipole–quadrupole* term, Eq. (14), with $+ \leftrightarrow -$ parity selection rules would account for the observed dipole-type preference for collisions of HCN with N_2. The results for collisions of HCN with He and Ar are again qualitatively similar and very different from all the other collisional cases. Since $\delta n_2/\delta n_1$ is negative, we would conclude that $k_{20} > k_{21}$ in Eq. (7), indicating a preference for quadrupole-type rotational transitions, i.e., quadrupole-type selection rules, $\Delta J = \pm 2$, or $\pm \leftrightarrow \pm$ parity selection rules. From Eqs. (11)–(14) and Table IV, we see that for collisions of HCN with He and Ar only the *dipole–dipole induced dipole* term applies, Eq. (13), with $\pm \leftrightarrow \pm$ parity selection rules, which would account for the observed quadrupole-type preference. Therefore we conclude that the observed collisional selection rules for rotational transitions are predominantly produced by *dipole–quadrupole* interactions for collisions of HCN with N_2, and by *dipole–dipole induced dipole* interactions for collisions of HCN with He and Ar.

Using the interaction potential terms above, we now discuss the differences between ion–neutral and neutral–neutral collisions which cause rotational transitions. First, we compare the collision–induced double resonance signals of HN_2^+ and HCN with He, as shown in Fig. 3. The difference between ion–neutral and neutral–neutral collisions for this case are dramatic. The zig-zag nature of the HCN–He collisional results demonstrate a strong preference for quadrupole-type rotational transitions, while the monotonically decreasing nature of the HN_2^+–He collisional results show a weaker preference for dipole-type rotational transitions. As we have just discussed above, the predominant interaction for collisions of HN_2^+ with He is the *dipole–charge induced dipole* interaction, while for collisions of HCN with He it is the *dipole–dipole induced dipole* interaction. Therefore we conclude that the ion–neutral and the neutral–neutral collisions which cause rotational transitions are different because of the presence of the *dipole–charge induced dipole* interaction in the ion–neutral collisions. This does not mean that the *dipole–dipole induced dipole* interaction is absent in the case of the ion–neutral collisions, but simply means that its contribution is small in comparison to the *dipole–charge induced dipole* interaction. Thus, the charge of the ion produces (i.e., the Langevin force) a charge induced dipole in He which interacts with the permanent dipole moment in HN_2^+. And this *dipole–charge induced dipole* interaction is the predominant interaction which produces the observed selection rules for collisions of HN_2^+ with He. The above discussion also applies to collisions of HN_2^+ and HCN with Ar.

The final comparison we would like to make is for the collision-induced double resonance of HN_2^+ and HCN with N_2 as shown in Fig. 4. Unlike the dramatic difference in the results shown in Fig. 3, the results shown in Fig. 4 are qualitatively very similar. From above, we note that the predominant interactions for collisions of HN_2^+ with N_2 are the *dipole–charge induced dipole* interaction and the *dipole–quadrupole* interaction, while for collisions of HCN with N_2 it is the *dipole–quadrupole* interaction. In this case, the ion–neutral and neutral–neutral collisions which cause rotational transitions exhibit the same collisional selection rules. The difference in the magnitude of the observed double resonance signals (cf. a factor of 2) is due to the additional presence of the *Langevin* term, Eq. (11), and the *dipole–charge induced dipole* term, Eq. (12), in the ion–neutral interaction potential (see Table IV). However, the *dipole–charge induced dipole* term will contribute to the observed selection rules, while the *Langevin* term will not contribute. The *Langevin* term itself does not cause rotational transitions of the molecular ion. Its effect is to exert an intermolecular force that is *always* attractive which reduces the ion–neutral distance. Thus the *Langevin* term causes the ion–neutral collisions to be stronger than neutral–neutral collisions and randomizes the rotational energy. The *Langevin* term is also the driving force for the proton transfer reaction, $HN_2^+ + N_2 \rightarrow N_2 + HN_2^+$, which also randomizes the rotational energy. Thus, in this case the ion–neutral and neutral–neutral collisions differ because of the presence of the Langevin term in the ion–neutral interaction potential, which reduces the preference for dipole-type transitions by a factor of 2.

TABLE IV. Interaction potential terms and selection rules for collisions of HN_2^+ and HCN with He, Ar, and N_2.

Potential Term	Selection Rules	Collisional Case	
		HN_2^+	HCN
V_L	⋯	He, Ar, N_2	⋯
$V_{\mu-\mu_c'}$	$+ \leftrightarrow -$, $\Delta J = \pm 1$	He, Ar, N_2	⋯
$V_{\mu-Q}$	$+ \leftrightarrow -$, $\Delta J = \pm 1$	N_2	N_2
$V_{\mu-\mu_d'}$	$\pm \leftrightarrow \pm$, $\Delta J = \pm 2$	He, Ar, N_2	He, Ar, N_2

IV. CONCLUSION

We have investigated collision-induced rotational transitions of HN_2^+ and HCN using infrared-microwave four-level double resonance spectroscopy. These two isoelectronic molecules were studied in collisions with He, Ar, and N_2. We have directly observed collisional selection rules, which has yielded information about the angular dependent part of the interaction potential.

For collision-induced double resonance of HN_2^+ with He, Ar, and N_2, we observed that the collisions exhibit a preference for dipole-type rotational transitions. These observed collisional dipole-type selection rules have been attributed to the *dipole–charge induced dipole* term in the interaction potential for collisions of HN_2^+ with He, Ar, and N_2, and also to the *dipole–quadrupole* term for collisions of HN_2^+ with N_2.

For collision-induced double resonance of HCN with He and Ar, we observed that the collisions exhibit a preference for quadrupole-type rotational transitions. These collisional quadrupole-type selection rules have been attributed to the *dipole–dipole induced dipole* term in the interaction potential for collisions of HCN with He and Ar. For collisions of HCN with N_2, a preference for dipole-type rotational transitions has been observed and attributed to the *dipole–quadrupole* term in the interaction potential.

This study has allowed us to directly compare the difference between ion–neutral and neutral–neutral collisions which cause rotational transitions. We have experimentally observed that ion–neutral and neutral–neutral collisions differ because of the presence of the Langevin force in the ion–neutral interaction potential, which has two unique effects. The Langevin force produces a charge-induced dipole in the collision partner which is parallel to the ion's electric field. This charge-induced dipole interacts with the electric charge of the molecular ion which creates an attractive force between the ion and neutral.[16] This interaction therefore decreases the ion–neutral distance and produces strong collisions which randomizes the rotational states. This is demonstrated by the collision-induced double resonance signals of HN_2^+ and HCN with N_2, where we have observed similar collisional selection rules, but have noted that the double resonance signals of the ion are two times smaller than those of the neutral. The second effect of the Langevin force occurs when the molecular ion has a permanent electric moment. The charge-induced dipole in the collision partner interacts with the electric moment of the molecular ion creating a long-range interaction. For a molecular ion with a permanent dipole moment, this interaction produces dipole-type collisional selection rules. This is demonstrated by the collision-induced double resonance signals of HN_2^+ with He and Ar which show a preference for dipole-type rotational transitions, while the double resonance signals of HCN with He and Ar show a remarkably different preference for quadrupole-type rotational transitions.

Note added in proof: After submission of this paper, we found a study of the pressure broadening of the $J = 1 \leftarrow 0$ transition of $HC^{15}N$ by nitrogen by Colmont.[26] He determined $\Delta\nu_p$ (HCN–N_2) = 6.58 MHz/Torr at 295 K. However, this does not change our argument in Sec. IV, where we estimated $\Delta\nu_p$ (HCN–N_2) $\approx$ 6 MHz/Torr at 300 K.

ACKNOWLEDGMENTS

This work has been supported by NSF Grants No. PHY 86-42211 and PHY 87-07025. We also acknowledge the partial support of the Petroleum Research Foundation administered by the American Chemical Society. D. P. Weliky gratefully acknowledges financial support from a McCormick Fellowship at The University of Chicago. We also thank K. Takagi for his contribution to the early stages of this work. This study has greatly benefited from C. S. Gudeman's thesis. We are indebted to his work on pressure broadened linewidths of molecular ions. We also thank R. C. Woods for helpful discussions, and the referee for useful comments.

[1] P. W. Anderson, Phys. Rev. **76,** 647 (1949).
[2] G. Birnbaum, Adv. Chem. Phys. **12,** 487 (1967).
[3] R. G. Gordon, W. Klemperer, and J. I. Steinfeld, Annu. Rev. Phys. Chem. **19,** 215 (1968).
[4] J. D. Lambert, *Vibrational and Rotational Relaxations in Gases* (Oxford, Clarendon, 1982).
[5] M. Faubel and J. P. Toennies, Adv. At. Mol. Phys. **13,** 229 (1977).
[6] A. J. McCafferty, M. J. Proctor, and B. J. Whitaker, Annu. Rev. Phys. Chem. **37,** 223 (1986).
[7] T. Oka, J. Chem. Phys. **45,** 752 (1966).
[8] T. Oka, Adv. At. Mol. Phys. **9,** 127 (1973).
[9] A. M. Ronn and E. B. Wilson, Jr., J. Chem. Phys. **46,** 3262 (1967); R. G. Gordon, P. E. Larson, C. H. Thomas, and E. B. Wilson, Jr., *ibid.* **50,** 1388 (1969); J. B. Cohen and E. B. Wilson, Jr., *ibid.* **58,** 442 (1973); S. L. Coy, *ibid.* **63,** 5145 (1975).
[10] T. Shimizu and T. Oka, J. Chem. Phys. **53,** 2536 (1970); Phys. Rev. A **2,** 1177 (1970).
[11] C. J. Pursell, D. P. Weliky, W. C. Ho, K. Takagi, and T. Oka, J. Chem. Phys. **91,** 7997 (1989).
[12] W. C. Ho, C. J. Pursell, D. P. Weliky, K. Takagi, and T. Oka, J. Chem. Phys. **93,** 87 (1990).
[13] S. Green, Astrophys. J. **201,** 366 (1975).
[14] S. Green and P. Thaddeus, Astrophys. J. **191,** 653 (1974).
[15] D. H. Katayama, Phys. Rev. Lett. **54,** 657 (1985).
[16] P. Langevin, Ann. Chim. Phys. **5,** 245 (1905).
[17] G. Gioumousis and D. P. Stevenson, J. Chem. Phys. **29,** 294 (1958).
[18] E. Herbst and W. Klemperer, Astrophys. J. **188,** 255 (1974).
[19] B. E. Turner, Astrophys. J. **193,** L83 (1974).
[20] T. A. Dixon and R. C. Woods, Phys. Rev. Lett. **34,** 61 (1975); R. C. Woods, T. A. Dixon, R. J. Saykally, and P. G. Szanto, *ibid.* **35,** 1269 (1975); R. J. Saykally, T. A. Dixon, T. G. Anderson, P. G. Szanto, and R. C. Woods, Astrophys. J. **205,** L101 (1976).
[21] T. G. Anderson, C. S. Gudeman, T. A. Dixon, and R. C. Woods, J. Chem. Phys. **72,** 1332 (1980).
[22] C. S. Gudeman, Ph. D. thesis, University of Wisconsin, Madison, 1982.
[23] S. Green and P. Thaddeus, Astrophys. J. **205,** 766 (1976).
[24] R. B. Nerf, J. Mol. Spectrosc. **58,** 479 (1975).
[25] C. H. Townes and A. L. Schawlow, *Microwave Spectroscopy* (Dover, New York, 1975), p. 364.
[26] J. M. Colmont, J. Mol. Spectrosc. **114,** 298 (1985).